Theoretical issues of small x physics [1]

J. Kwieciński
Department of Physics
University of Durham
Durham, UK
and
Department of Theoretical Physics
H. Niewodniczański Institute of Nuclear Physics
Kraków, Poland. [2]

arXiv:hep-ph/9602286v1 13 Feb 1996

Abstract

The perturbative QCD predictions concerning deep inelastic scattering at low x are summarized. The theoretical framework based on the leading log $1/x$ resummation and k_t factorization theorem is described and some recent developments concerning the BFKL equation and its generalization are discussed. The QCD expectations concerning the small x behaviour of the spin dependent structure function $g_1(x, Q^2)$ are briefly summarized and the importance of the double logarithmic terms which sum contributions containing the leading powers of $\alpha_s ln^2(1/x)$ is emphasised. The role of studying final states in deep inelastic scattering for revealing the details of the underlying dynamics at low x is pointed out and some dedicated measurements, like deep inelastic scattering accompanied by an energetic jet, the measurement of the transverse energy flow etc., are briefly discussed.

[1] An introductory review talk given at the UK Phenomenology Workshop on HERA Physics, St. John's College, Durham, UK, September 1995

[2] Permanent address

Perturbative QCD predicts that several new phenomena will occur when the parameter x specifying the longitudinal momentum fraction of a hadron carried by a parton (i.e. by a quark or by a gluon) becomes very small [1, 2] . The main expectation is that the gluon densities should strongly grow in this limit, eventually leading to the parton saturation effects [1, 2, 3, 4]. The small x behaviour of the structure functions is driven by the gluon through the $g \to q\bar{q}$ transition and the increase of gluon distributions with decreasing x implies a similar increase of the deep inelastic lepton - proton scattering structure function F_2 as the Bjorken parameter x decreases [7]. The Bjorken parameter x is, as usual, defined as $x = Q^2/(2pq)$ where p is the proton four momentum, q the four momentum transfer between the leptons and $Q^2 = -q^2$. The recent experimental data are consistent with this perturbative QCD prediction that the structure function $F_2(x, Q^2)$ should strongly grow with the decreasing Bjorken parameter x [8, 9].

The growth of structure functions with decreasing parameter x is much stronger than that which would follow from the expectations based on the "soft" pomeron exchange mechanism with the soft pomeron intercept $\alpha_{soft} \approx 1.08$ as determined from the phenomenological analysis of total hadronic and real photoproduction cross-sections [10].

Small x behaviour of structure functions for fixed Q^2 reflects the high energy behaviour of the virtual Compton scattering total cross-section with increasing total CM energy squared W^2 since $W^2 = Q^2(1/x - 1)$. The Regge pole exchange picture [11] would therefore appear quite appropriate for the theoretical description of this behaviour.

The high energy behaviour of the total hadronic and (real) photoproduction cross-sections can be economically described by two contributions: an (effective) pomeron with its intercept slightly above unity (~ 1.08) and the leading meson Regge trajectories with intercept $\alpha_R(0) \approx 0.5$ [10]. The reggeons can be identified as corresponding to ρ, ω, f or A_2 exchange(s) depending upon the quantum numbers involved. All these reggeons have approximately the same intercept. One refers to the pomeron obtained from the phenomenological analysis of hadronic total cross sections as the "soft" pomeron since the bulk of the processes building-up the cross sections are low p_t (soft) processes.

The Regge pole model gives the following parametrization of the deep inelastic scattering structure function $F_2(x, Q^2)$ at small x

$$F_2(x, Q^2) = \sum_i \tilde{\beta}_i(Q^2) x^{1-\alpha_i(0)}. \tag{1}$$

The relevant reggeons are those which can couple to two (virtual) photons. The (singlet) part of the structure function F_2 is controlled at small x by pomeron exchange, while the non-singlet part $F_2^{NS} = F_2^p - F_2^n$ by the A_2 reggeon. Neither pomeron nor A_2 reggeons couple to the spin structure function $g_1(x, Q^2)$ which is described at small x by the exchange of reggeons corresponding to axial vector mesons [12, 13] i.e. to A_1 exchange for the non-singlet part $g_1^{NS} = g_1^p - g_1^n$ etc.

$$g_1^{NS}(x, Q^2) = \gamma(Q^2) x^{-\alpha_{A_1}(0)}. \tag{2}$$

The reggeons which correspond to axial vector mesons are expected to have very low intercept (i.e. $\alpha_{A_1} \leq 0$ etc.).

The high energy behaviour which follows from perturbative QCD is often refered to as being related to the "hard" pomeron in contrast to the soft pomeron describing the high energy behaviour of hadronic and photoproduction cross-sections.

In Fig. 1 we summarize the present experimental situation on the variation of the total virtual Compton scattering cross-section with total CM energy W for different photon virtualities Q^2 which range from the real photoproduction ($Q^2 = 0$) to the deep inelastic region [15]. The change of high energy behaviour with the scale Q^2 is evidently present in the data.

The purpose of this talk is to review some of the recent theoretical developments concerning deep inelastic scattering in the limit of small x. The next section is devoted to the discussion of the BFKL equation which resums the leading powers of $ln(1/x)$ and to the unified evolution equation [16, 17, 18, 19] based on coherence and angular ordering [20]. The k_t factorization theorem [21, 22, 23], its connection with collinear factorization as well as the small x resummation effects within the QCD evolution formalism are also discussed in this section. In sec. 3 we present the theoretical expectation for the small x behaviour of the spin dependent structure function $g_1(x, Q^2)$ concentrating for simplicity on its non-singlet part. The novel feature in this case is importance of the double logarithmic terms i.e. of those terms in the perturbative expansion which contain powers of $\alpha_s ln^2(1/x)$. Finally in sec. 4 we discuss some of the dedicated measurements like deep inelastic + jet events and transverse energy flow etc. which aim at revealing the dynamical details of small x physics. Sec. 5 contains a brief summary and outlook.

2. The BFKL pomeron and QCD predictions for the small x behaviour of the structure function F_2

At small x the dominant role is played by the gluons and the basic dynamical quantity is the unintegrated gluon distribution $f(x, Q_t^2)$ where x denotes the momentum fraction of a parent hadron carried by a gluon and Q_t its transverse momentum. The unintegrated distribution $f(x, Q_t^2)$ is related in the following way to the more familiar scale dependent gluon distribution $g(x, Q^2)$:

$$xg(x, Q^2) = \int^{Q^2} \frac{dQ_t^2}{Q_t^2} f(x, Q_t^2). \tag{3}$$

In the leading $ln(1/x)$ approximation the unintegrated distribution $f(x, Q_t^2)$ satisfies the BFKL equation [5, 6, 16] which has the following form:

$$f(x, Q_t^2) = f^0(x, Q_t^2) +$$

$$\bar{\alpha}_s \int_x^1 \frac{dx'}{x'} \int \frac{d^2q}{\pi q^2} \left[\frac{Q_t^2}{(\boldsymbol{q} + \boldsymbol{Q_t})^2} f(x', (\boldsymbol{q} + \boldsymbol{Q_t})^2) - f(x', Q_t^2)\Theta(Q_t^2 - q^2) \right] \tag{4}$$

where

$$\bar{\alpha}_s = \frac{3\alpha_s}{\pi} \tag{5}$$

The first and the second terms on the right hand side of eq. (4) correspond to real gluon emission with q being the transverse momentum of the emitted gluon, and to the virtual

corrections respectively. $f^0(x,Q_t^2)$ is a suitably defined inhomogeneous term.

After resumming the virtual corrections and "unresolvable" gluon emissions ($q^2 < \mu^2$) where μ is the resolution defining the "resolvable" radiation, equation (4) can be rearranged into the following "folded" form:

$$f(x,Q_t^2) = \hat{f}^0(x,Q_t^2) +$$

$$\bar{\alpha}_s \int_x^1 \frac{dx'}{x'} \int \frac{d^2q}{\pi q^2} \Theta(q^2-\mu^2) \Delta_R(\frac{x}{x'},Q_t^2) \frac{Q_t^2}{(\boldsymbol{q}+\boldsymbol{Q_t})^2} f(x',(\boldsymbol{q}+\boldsymbol{Q_t})^2) + O(\mu^2/Q_t^2) \quad (6)$$

where Δ_R which screens the $1/z$ singularity is given by:

$$\Delta_R(z,Q_t^2) = z^{\bar{\alpha}_s ln(Q_t^2/\mu^2)} = exp\left(-\bar{\alpha}_s \int_z^1 \frac{dz'}{z'} \int_{\mu^2}^{Q_t^2} \frac{dq^2}{q^2}\right) \quad (7)$$

and

$$\hat{f}^0(x,Q_t^2) = \int_x^1 \frac{dx'}{x'} \Delta_R(\frac{x}{x'},Q_t^2) \frac{df^0(x',Q_t^2)}{dln(1/x')} \quad (8)$$

Equation (6) sums the ladder diagrams (see Fig. 2) with the reggeized gluon exchange along the chain with the gluon trajectory $\alpha_G(Q_t^2) = 1 - \frac{\bar{\alpha}_s}{2} ln(Q_t^2/\mu^2)$.

For the fixed coupling case eq. (4) can be solved analytically and the leading behaviour of its solution at small x is given by the following expression:

$$f(x,Q_t^2) \sim (Q_t^2)^{\frac{1}{2}} \frac{x^{-\lambda_{BFKL}}}{\sqrt{ln(\frac{1}{x})}} exp\left(-\frac{ln^2(Q_t^2/\bar{Q}^2)}{2\lambda" ln(1/x)}\right) \quad (9)$$

with

$$\lambda_{BFKL} = 4ln(2)\bar{\alpha}_s \quad (10)$$

$$\lambda" = \bar{\alpha}_s 28\zeta(3) \quad (11)$$

where the Riemann zeta function $\zeta(3) \approx 1.202$. The parameter $\bar{Q}$ is of nonperturbative origin.

The quantity $1+\lambda_{BFKL}$ is equal to the intercept of the so - called BFKL pomeron. Its potentially large magnitude (~ 1.5) should be contrasted with the intercept $\alpha_{soft} \approx 1.08$ of the (effective) "soft" pomeron which has been determined from the phenomenological analysis of the high energy behaviour of hadronic and photoproduction total cross-sections [10].

The solution of the BFKL equation reflects its diffusion pattern which is the direct consequence of the absence of transverse momentum ordering along the gluon chain. In this respect the BFKL dynamics is different from that based on the (leading order) Altarelli-Parisi evolution which corresponds to strongly - ordered transverse momenta. The interrelation between the diffusion of transverse momenta towards both the infrared and ultraviolet regions **and** the increase of gluon distributions with decreasing x is a characteristic property of QCD at low x. It has important consequences for the structure of the hadronic final state in deep inelastic scattering at small x.

In practice one introduces the running coupling $\bar{\alpha}_s(Q_t^2)$ in the BFKL equation (4). This requires the introduction of an infrared cut-off to prevent entering the infrared region where the coupling becomes large. The effective intercept λ_{BFKL} found by numerically solving the equation depends weakly on the magnitude of this cut-off [25]. The impact of the momentum cut-offs on the solution of the BFKL equation has also been discussed in refs. [26, 27].

The solution (9) of the BFKL equation is obtained most directly by solving the corresponding equation for the moment function

$$\bar{f}(\omega, Q_t^2) = \int_0^1 \frac{dx}{x} x^\omega f(x, q_t^2) \tag{12}$$

$$\bar{f}(\omega, Q_t^2) = \bar{f}^0(\omega, Q_t^2) + \frac{\bar{\alpha}_s}{\omega} \int \frac{d^2q}{\pi q^2} \left[\frac{Q_t^2}{(\boldsymbol{q} + \boldsymbol{Q_t})^2} \bar{f}(\omega, (\boldsymbol{q} + \boldsymbol{Q_t})^2) - \bar{f}(\omega, Q_t^2) \Theta(Q_t^2 - q^2) \right] \tag{13}$$

This equation can be diagonalised by a Mellin transform. The solution for the Mellin transform $\tilde{f}(\omega, \gamma)$ of the moment function $\bar{f}(\omega, Q_t^2)$ is:

$$\tilde{f}(\omega, \gamma) = \frac{\tilde{f}^0(\omega, \gamma)}{1 - \frac{\bar{\alpha}_s}{\omega} \tilde{K}(\gamma)} \tag{14}$$

where

$$\tilde{K}(\gamma) = 2\Psi(1) - \Psi(\gamma) - \Psi(1 - \gamma) \tag{15}$$

is the Mellin transform of the kernel of eq. (13). The function $\Psi(z)$ is the logarithmic derivative of the Euler Γ function. The Mellin transform $\tilde{f}(\omega, \gamma)$ is defined by:

$$\tilde{f}(\omega, \gamma) = \int_0^\infty \frac{dQ_t^2}{Q_t^2} (Q_t^2)^{-\gamma} \bar{f}(\omega, Q_t^2), \tag{16}$$

and hence the function $\bar{f}(\omega, Q_t^2)$ is related to $\tilde{f}(\omega, \gamma)$ through the inverse Mellin transform

$$\bar{f}(\omega, Q_t^2) = \frac{1}{2\pi i} \int_{1/2-i\infty}^{1/2+i\infty} d\gamma (Q_t^2)^\gamma \tilde{f}(\omega, \gamma). \tag{17}$$

The poles of $\tilde{f}(\omega, \gamma)$ in the γ plane define the anomalous dimensions of the moment function $\bar{f}(\omega, Q_t^2)$ [24]. The (leading twist) anomalous dimension $\gamma_{gg}(\omega, \bar{\alpha}_s)$ of $\bar{f}(\omega, Q_t^2)$ gives the following behaviour of $\bar{f}(\omega, Q_t^2)$ at large Q_t^2

$$\bar{f}(\omega, Q_t^2) = \tilde{f}^0(\omega, \gamma = \gamma_{gg}(\omega, \bar{\alpha}_s)) \gamma_{gg}(\omega, \bar{\alpha}_s) R(\alpha_s, \omega) (Q_t^2)^{\gamma_{gg}(\omega, \bar{\alpha}_s)} \tag{18}$$

where

$$R(\alpha_s, \omega) = - \left[\frac{\bar{\alpha}_s}{\omega} \gamma_{gg}(\omega, \bar{\alpha}_s) \frac{d\tilde{K}(\gamma)}{d\gamma} \Big|_{\gamma = \gamma_{gg}(\omega, \bar{\alpha}_s)} \right]^{-1}. \tag{19}$$

The anomalous dimension will also, of course, control the large Q^2 behaviour of the moment function $\bar{g}(\omega, Q^2)$ of the integrated gluon distribution

$$\bar{g}(\omega, Q^2) = \int_0^{Q^2} \frac{dQ_t^2}{Q_t^2} f(\omega, Q_t^2) \tag{20}$$

which has the following form:

$$\bar{g}(\omega, Q^2) = R(\alpha_s, \omega)\bar{g}^0(\omega)\left(\frac{Q^2}{Q_0^2}\right)^{\gamma_{gg}(\omega,\bar{\alpha}_s)} \tag{21}$$

where we have introduced the moment function of the input distribution

$$\bar{g}^0(\omega) = \tilde{f}^0(\omega, \gamma = \gamma_{gg}(\omega, \bar{\alpha}_s))(Q_0^2)^{\gamma_{gg}(\omega,\bar{\alpha}_s)}. \tag{22}$$

Equations (21)and (22) follow directly from equations (18), (19) and (20). It may be seen from eq. (21) that the BFKL singularity affects the "starting" gluon distribution at $Q^2 = Q_0^2$ through the factor R [22].

It follows from eq.(15) that the anomalous dimension $\gamma_{gg}(\omega, \bar{\alpha}_s))$ is the solution of the following equation:

$$\frac{\bar{\alpha}_s}{\omega}\tilde{K}(\gamma_{gg}(\omega, \bar{\alpha}_s)) = 1. \tag{23}$$

It is a function of only one variable $\frac{\bar{\alpha}_s}{\omega}$ i.e. $\gamma_{gg}(\omega, \bar{\alpha}_s) \to \gamma_{gg}(\frac{\bar{\alpha}_s}{\omega})$. The solution of eq. (23) makes it possible to obtain the anomalous dimension $\gamma_{gg}(\frac{\bar{\alpha}_s}{\omega})$ as a power series of $\frac{\bar{\alpha}_s}{\omega}$ [24]

$$\gamma_{gg}(\frac{\bar{\alpha}_s}{\omega}) = \sum_{n=1}^{\infty} c_n \left(\frac{\bar{\alpha}_s}{\omega}\right)^n. \tag{24}$$

This power series corresponds to the leading $ln(1/z)$ expansion of the splitting function $P_{gg}(z, \alpha_s)$

$$zP_{gg}(z, \alpha_s) = \bar{\alpha}_s \sum_{n=1}^{\infty} c_n \frac{(\bar{\alpha}_s ln(1/z))^{n-1}}{(n-1)!} \tag{25}$$

which controls the evolution of the gluon distribution.

The structure functions $F_{2,L}(x, Q^2)$ are described at small x by the diagram of Fig.3 which gives the following relation between the structure functions and the unintegrated distribution f:

$$F_{2,L}(x, Q^2) = \int_x^1 \frac{dx'}{x'} \int \frac{dQ_t^2}{Q_t^2} F_{2,L}^{box}(x', Q_t^2, Q^2) f(\frac{x}{x'}, Q_t^2). \tag{26}$$

The functions $F_{2,L}^{box}(x', Q_t^2, Q^2)$ may be regarded as the structure functions of the off-shell gluons with virtuality Q_t^2. They are described by the quark box (and crossed box) diagram contributions to the photon-gluon interaction in the upper part of the diagram of Fig. 3. The small x behaviour of the structure functions reflects the small z ($z = x/x'$) behaviour of the gluon distribution $f(z, Q_t^2)$.

Equation (26) is an example of the "k_t factorization theorem" which relates measurable quantities (like DIS structure functions) to the convolution in both longitudinal as well as in transverse momenta of the universal gluon distribution $f(z, Q_t^2)$ with the cross-section (or structure function) describing the interaction of the "off-shell" gluon with the hard probe [22, 21]. The k_t factorization theorem is the basic tool for calculating the observable quantities in the small x region in terms of the (unintegrated) gluon distribution f which is the solution of the BFKL equation.

The leading - twist part of the k_t factorization formula can be rewritten in a collinear factorization form. The leading small x effects are then automatically resummed in the splitting functions and in the coefficient functions. The k_t factorization theorem can in fact be used as the tool for calculating these quantities. Thus, for instance, the moment function $\bar{P}_{qg}(\omega, \alpha_s)$ of the splitting function is represented in the following form (in the DIS scheme):

$$\bar{P}_{qg}(\omega, \alpha_s) = \frac{\gamma_{gg}^2(\frac{\bar{\alpha}_s}{\omega})\tilde{F}_2^{box}\left(\omega = 0, \gamma = \gamma_{gg}(\frac{\bar{\alpha}_s}{\omega})\right)}{2\sum_i e_i^2} \tag{27}$$

where $\tilde{F}_2^{box}(\omega, \gamma)$ is the Mellin transform of the moment function $\bar{F}_2^{box}(\omega, Q_t^2, Q^2)$ i.e.

$$\bar{F}_2^{box}(\omega, Q_t^2, Q^2) = \frac{1}{2\pi i}\int_{1/2-i\infty}^{1/2+i\infty} d\gamma \tilde{F}_2^{box}(\omega, \gamma)\left(\frac{Q^2}{Q_t^2}\right)^{\gamma} \tag{28}$$

Representation (27) generates the following expansion of the splitting function $P_{qg}(z, \alpha_s)$ at small z:

$$zP_{qg}(z, \alpha_s) = \frac{\alpha_s}{2\pi} zP^{(0)}(z) + (\bar{\alpha}_s)^2 \sum_{n=1}^{\infty} b_n \frac{[\bar{\alpha}_s ln(1/z)]^{n-1}}{(n-1)!} \tag{29}$$

The first term on the right hand side of eq. (29) vanishes at $z = 0$. It should be noted that the splitting function P_{qg} is formally non-leading at small z when compared with the splitting function P_{gg} . For moderately small values of z however, when the first few terms in the expansions (24) and (29) dominate, the BFKL effects can be much more important in P_{qg} than in P_{gg}. This comes from the fact that in the expansion (29) all coefficients b_n are different from zero while in eq. (24) we have $c_2 = c_3 = 0$ [24]. The small x resummation effects within the conventional QCD evolution formalism have recently been discussed in refs. [28, 29, 30, 31]. In Fig. 4 we show the results of this analysis for the structure function $F_2(x, Q^2)$ [29] where the starting parton distributions have been assumed to be non-singular. In this figure we compare the standard two-loop results (dashed curves) with those which contain the leading $ln(1/x)$ resummations. The dot-dashed curve corresponds to keeping the small x corrections only in the gluon anomalous dimension while the solid and dotted curves show the effect of including the small x resummation in the splitting function P_{qg} as well. (The two curves were obtained by applying two different prescriptions of implementing the momentum sum rule which is violated in the $LL1/x$ approximation). One can see from this figure that at the moderately small values of x which are relevant for the HERA measurements, the small x resummation effects in the splitting function P_{qg} have a much stronger impact on F_2 than the small x resummation in the splitting function P_{gg}. This reflects the fact, which has already been mentioned above, that in the expansion (29) all coefficients b_n are different from zero while in eq. (24) we have $c_2 = c_3 = 0$.

A more general treatment of the gluon ladder than that which follows from the BFKL formalism is provided by the CCFM equation based on angular ordering along the gluon chain [17, 18]. This equation embodies both the BFKL equation at small x and the conventional Altarelli-Parisi evolution at large x. The unintegrated gluon distribution f now acquires dependence upon an additional scale Q which specifies the maximal angle of gluon emission. The CCFM equation has a form analogous to that of the "folded" BFKL equation (6):

$$f(x, Q_t^2, Q^2) = \hat{f}^0(x, Q_t^2, Q^2) +$$

$$\bar{\alpha}_s \int_x^1 \frac{dx'}{x'} \int \frac{d^2q}{\pi q^2} \Theta(Q - qx/x') \Delta_R(\frac{x}{x'}, Q_t^2, q^2) \frac{Q_t^2}{(\boldsymbol{q} + \boldsymbol{Q_t})^2} f(x', (\boldsymbol{q} + \boldsymbol{Q_t})^2, q^2)) \qquad (30)$$

where the theta function $\Theta(Q - qx/x')$ reflects the angular ordering constraint on the emitted gluon. The "non-Sudakov" form-factor $\Delta_R(z, Q_t^2, q^2)$ is now given by the following formula:

$$\Delta_R(z, Q_t^2, q^2) = exp\left[-\bar{\alpha}_s \int_z^1 \frac{dz'}{z'} \int \frac{dq'^2}{q'^2} \Theta(q'^2 - (qz')^2) \Theta(Q_t^2 - q'^2)\right] \qquad (31)$$

Eq.(30) still contains only the singular term of the $g \to gg$ splitting function at small z. Its generalization which would include remaining parts of this vertex (as well as quarks) is possible. The numerical analysis of this equation was presented in ref. [18].

In Fig. 5 we show the results for the structure function F_2 calculated from the k_t factorization theorem using the function f obtained from the CCFM equation [32]. We confront these predictions with the most recent data from the H1 and ZEUS collaborations at HERA [8, 9] as well as with the results of the analysis which was based on the Altarelli-Parisi equation alone without the small x resummation effects being included in the formalism [33, 34]. In the latter case the singular small x behaviour of the gluon and sea quark distributions has to be introduced in the parametrization of the starting distributions at the moderately large reference scale $Q^2 = Q_0^2$ (i.e. $Q_0^2 \approx 4GeV^2$ or so) [33]. One can also generate steep behaviour dynamically starting from non-singular "valence-like" parton distributions at some very low scale $Q_0^2 = 0.35GeV^2$ [34]. In the latter case the gluon and sea quark distributions exhibit "double logarithmic behaviour" [35]

$$F_2(x, Q^2) \sim exp\left(2\sqrt{\xi(Q^2, Q_0^2) ln(1/x)}\right) \qquad (32)$$

where

$$\xi(Q^2, Q_0^2) = \int_{Q_0^2}^{Q^2} \frac{dq^2}{q^2} \frac{3\alpha_s(q^2)}{\pi}. \qquad (33)$$

For very small values of the scale Q_0^2 the evolution length $\xi(Q^2, Q_0^2)$ can become large for moderate and large values of Q^2 and the "double logarithmic" behaviour (32) is, within the limited region of x, similar to that corresponding to the power like increase of the type $x^{-\lambda}$, $\lambda \approx 0.3$. This explains similarity between the theoretical curves presented in Fig. 5. The theoretical results also show that an inclusive quantity like F_2 is not the best discriminator for revealing the dynamical details at low x. One may however hope that this can be provided by studying the structure of the hadronic final state in deep inelastic scattering and this possibility will be briefly discussed in sec. 4.

Although the BFKL and CCFM equations for the gluon distribution become equivalent in the leading $ln(1/x)$ approximation they begin to differ if less inclusive quantities are considered. In the case of the observables which are not infrared safe (like multiplicity of jets etc.) the CCFM formalism generates double logarithmic $ln(1/x)$ terms i.e. terms which contain powers of $\alpha_s ln^2(1/x)$. This is of course closely related to the fact that the angular ordering constraint serves also as the infrared regulator and so the transverse momentum integrations generate additional powers of $ln(1/x)$ besides the "conventional" ones which come from the integration over the longitudinal momenta. Also the virtual corrections contain double logarithmic terms as well. This can easily be seen from the definition of the "non-Sudakov" form factor (31). The double logarithmic terms exactly

cancel between the real emission contributions and virtual corrections to the gluon distribution but remain present in the less inclusive quantities. On the other hand in the BFKL case only the single logarithmic terms (i.e. powers of $\alpha_s ln(1/x)$) are present in all quantities but the observables which are not infrared safe diverge for $\mu^2 \to 0$ where μ is the resolution parameter. The gluon distribution itself remains of course finite in this limit.

Several new interesting results have been obtained in the formal studies of the high energy (or small x) limit in QCD which go beyond the leading logarithmic approximation [6, 36, 37, 43, 44]. The important theoretical tool in this case is the effective field theory where the basic objects are the reggeized gluons and the effective action of this effective field theory obeys conformal invariance [36, 37]. Theoretical analysis simplifies in the large N_c limit. One can discuss both the pomeron which appears as the bound state of two (reggeized) gluons, and the odderon (i.e. the bound state of three reggeized gluons), as well as bound states of many reggeized gluons [38]. Conformal invariance is also very useful for analysing the BFKL pomeron away from the forward direction [39, 40] as well as the the triple pomeron and more complicated vertices [41].

The genuine next-to-leading $\ln(1/x)$ corrections to the BFKL equation can be present in all relevant quantities i.e. in the particle-particle-reggeon vertex, the reggeon-reggeon-particle vertex and in the gluon Regge trajectory [43, 44]. (The reggeon here corresponds to the reggeized gluon). Besides that one has also to include additional region of phase-space which goes beyond strong ordering of longitudinal momenta.

It should finally be emphasised that in impact parameter representation the BFKL equation offers an interesting interpretation in terms of colour dipoles [42].

4. Small x behaviour of the nonsignlet unpolarized and polarized structure functions

The discussion presented in the previous Section concerned the small x behaviour of the singlet structure function which was driven by the gluon through the $g \to q\bar{q}$ transition. The gluons of course decouple from the non-singlet channel and the mechanism of generating the small x behaviour in this case is different.

The simple Regge pole exchange model predicts in this case that

$$F_2^{NS}(x, Q^2) = F_2^p(x, Q^2) - F_2^n(x, Q^2) \sim x^{1-\alpha_{A_2}(0)} \tag{34}$$

where $\alpha_{A_2}(0)$ is the intercept of the A_2 Regge trajectory. For $\alpha_{A_2}(0) \approx 1/2$ this behaviour is stable against leading order QCD evolution. This follows from the fact that the leading singularity of the moment $\gamma_{qq}(\omega)$ of the splitting function $P_{qq}(z)$:

$$\gamma(\omega) = \int_0^1 \frac{dz}{z} z^\omega P_{qq}(z) \tag{35}$$

is located at $\omega = 0$ and so the (nonperturbative) A_2 Regge pole at $\omega = \alpha_{A_2}(0) \approx 1/2$ remains the leading singularity controlling the small x behaviour of the non-singlet structure function.

The novel feature of the non-singlet channel is the appearence of the **double** logarithmic terms i.e. powers of $\alpha_s ln^2(1/x)$ at each order of the perturbative expansion [45, 46, 47, 48, 49]. These double logarithmic terms are generated by the ladder diagrams with quark (antiquark) exchange along the chain. The ladder diagrams can acquire corrections from the "bremsstrahlung" contributions [47, 49] which do not vanish for the polarized structure function $g_1^{NS}(x,Q^2)$ [49].

In the approximation where the leading double logarithmic terms are generated by ladder diagrams illustrated in Fig. 6 the unintegrated non-singlet quark distribution $f_q^{NS}(x,k_t^2)$ ($q^{NS}=u+\bar{u}-d-\bar{d}$) satisfies the following integral equation :

$$f_q^{NS}(x,Q_t^2)=f_{q0}^{NS}(x,Q_t^2)+\tilde{\alpha}_s\int_x^1\frac{dz}{z}\int_{Q_0^2}^{\frac{Q_t^2}{z}}\frac{dQ_t'^2}{Q_t'^2}f_q^{NS}(\frac{x}{z},Q_t'^2) \tag{36}$$

where

$$\tilde{\alpha}_s=\frac{2}{3\pi}\alpha_s \tag{37}$$

and Q_0^2 is the infrared cut-off parameter. The unintegrated distribution $f_q^{NS}(x,Q_t^2)$ is, as usual, related in the following way to the scale dependent (nonsinglet) quark distribution $q^{NS}(x,Q^2)$:

$$q^{NS}(x,Q^2)=\int^{Q^2}\frac{dQ_t^2}{Q_t^2}f_q^{NS}(x,Q_t^2). \tag{38}$$

The upper limit Q_t^2/z in the integral equation (36) follows from the requirement that the virtuality of the quark at the end of the chain is dominated by Q_t^2. A possible non-perturbative A_2 reggeon contribution has to be introduced in the driving term i.e.

$$f_{q0}^{NS}(x,Q_t^2)\sim x^{-\alpha_{A_2}(0)} \tag{39}$$

at small x.

Equation (36) implies the following equation for the moment function $\bar{f}_q^{NS}(\omega,Q_t^2)$

$$\bar{f}_q^{NS}(\omega,Q_t^2)=\bar{f}_{q0}^{NS}(\omega,Q_t^2)+\frac{\tilde{\alpha}_s}{\omega}\left[\int_{Q_0^2}^{Q_t^2}\frac{dQ_t'^2}{Q_t'^2}\bar{f}_q^{NS}(\omega,Q_t'^2)+\int_{Q_t^2}^{\infty}\frac{dQ_t'^2}{Q_t'^2}\left(\frac{Q_t^2}{Q_t'^2}\right)^{\omega}\bar{f}_q^{NS}(\omega,Q_t'^2)\right] \tag{40}$$

Equation (40) follows from (36) after taking into account the following relation:

$$\int_0^1\frac{dz}{z}z^{\omega}\Theta\left(\frac{Q_t^2}{Q_t'^2}-z\right)=\frac{1}{\omega}\left[\Theta(Q_t^2-Q_t'^2)+\left(\frac{Q_t^2}{Q_t'^2}\right)^{\omega}\Theta(Q_t'^2-Q_t^2)\right]. \tag{41}$$

For fixed coupling $\tilde{\alpha}_s$ equation (40) can be solved analytically. Assuming for simplicity that the inhomogeneous term is independent of Q_t^2 (i.e. that $\bar{f}_{q0}^{NS}(\omega,Q_t^2)=C(\omega)$) we get the following solution of eq.(40):

$$\bar{f}_q^{NS}(\omega,Q_t^2)=C(\omega)R(\tilde{\alpha}_s,\omega)\left(\frac{Q_t^2}{Q_0^2}\right)^{\gamma^-(\tilde{\alpha}_s,\omega)} \tag{42}$$

where

$$\gamma^-(\tilde{\alpha}_s,\omega)=\frac{\omega-\sqrt{\omega^2-4\tilde{\alpha}_s}}{2} \tag{43}$$

and

$$R(\tilde{\alpha}_s,\omega)=\frac{\omega\gamma^-(\tilde{\alpha}_s,\omega)}{\tilde{\alpha}_s}. \tag{44}$$

Equation (43) defines the anomalous dimension of the moment of the non-singlet quark distribution in which the double logarithmic $ln(1/x)$ terms i.e. the powers of $\frac{\alpha_s}{\omega^2}$ have been resummed to all orders. It can be seen from (43) that this anomalous dimension has a (square root) branch point singularity at $\omega=\bar{\omega}$ where

$$\bar{\omega}=2\sqrt{\tilde{\alpha}_s}. \tag{45}$$

This singularity will of course be also present in the moment function $\bar{f}_q^{NS}(\omega,Q_t^2)$ itself. It should be noted that in contrast to the BFKL singularity whose position above unity was proportional to α_s, $\bar{\omega}$ is proportional to $\sqrt{\alpha_s}$ - this being the straightforward consequence of the fact that equation (40) sums double logarithmic terms $(\frac{\alpha_s}{\omega^2})^n$. This singularity gives the following contribution to the non-singlet quark distribution $f_q^{NS}(x,Q_t^2)$ at small x:

$$f_q^{NS}(x,Q_t^2)\sim\frac{x^{-\bar{\omega}}}{ln^{3/2}(1/x)}. \tag{46}$$

For small values of the QCD coupling this contribution remains non - leading in comparison to the contribution of the A_2 Regge pole.

As has been mentioned above the corresponding integral equation which resums the double logarithmic terms in the spin dependent quark distributions is more complicated than the simple ladder equation (36) due to non-vanishing contributions coming from bremsstrahlung diagrams. It may however be shown that , at least as far as the non-singlet structure function is concerned, these contributions give only a relatively small correction to $\bar{\omega}$. The main interest in applying the QCD evolution equations to study the spin structure function is that the naive Regge pole expectations based on the exchange of low-lying Regge trajectories become unstable against the QCD perturbative "corrections". The relevant reggeon which contributes to $g_1^{NS}(x,Q^2)$ is the A_1 exchange which is expected to have a very low intercept $\alpha_{A_1}(0)\leq 0$. The perturbative singularity generated by the double logarithmic $ln(1/x)$ resummation can therefore become much more important than in the case of the unpolarized case where it is hidden behind leading A_2 exchange contribution. Even if we restrict ourselves to leading order QCD evolution [50, 51] then the non-singular $x^{-\alpha_{A_1}(0)}$ behaviour (with $\alpha_{A_1}(0)\leq 0$) becomes unstable as well and the polarized quark densities acquire singular behaviour:

$$\Delta q^{NS}(x,Q^2)\sim exp(2\sqrt{\xi^{NS}(Q^2)ln(1/x)}) \tag{47}$$

where

$$\xi^{NS}(Q^2)=\int^{Q^2}\frac{dq^2}{q^2}\tilde{\alpha}_s(q^2) \tag{48}$$

This follows from the fact that $\Delta P_{qq}(z)=P_{qq}(z)$ where $P_{qq}(z)$ and $\Delta P_{qq}(z)$ are the splitting functions describing the evolution of the spin independent and spin dependent quark distributions respectively and from the fact that $P_{qq}(z)\to const$ as $z\to 0$.

The introduction of the running coupling effects in equation (40) turns the branch point singularity into the series of poles which accumulate at $\omega=0$ [46]. The numerical

analysis of the corresponding integral equation, with the running coupling effects taken into account, gives an effective slope ,

$$\lambda(x, Q_t^2) = \frac{dln\Delta f_q^{NS}(x, Q_t^2)}{dln(1/x)} \tag{49}$$

with magnitude $\lambda(x, Q_t^2) \approx 0.2 - 0.3$ at small x [52]. The result of this estimate suggest that a reasonable extrapolation of the (non-singlet) polarized quark densities would be to assume an $x^{-\lambda}$ behaviour with $\lambda \approx 0.2 - 0.3$. Similar extrapolations of the spin-dependent quark distributions towards the small x region have been assumed in several recent parametrizations of parton densities [53, 54, 55, 56]. The small x behaviour of the spin dependent structure function g_1 has also been disscussed in refs. [57, 58].

5. The structure of the hadronic final state in deep inelastic scattering at low x

It is expected that absence of transverse momentum ordering along the gluon chain, which leads to the correlation between the increase of the structure function with decreasing x and the diffusion of transverse momentum should reflect itself in the behaviour of less inclusive quantities than the structure function $F_2(x, Q^2)$. The dedicated measurements of low x physics which are particularly sensitive to this correlation are the deep inelastic plus jet events, transverse energy flow in deep inelastic scattering, production of jets separated by the large rapidity gap and dijet production in deep inelastic scattering. The diagrammatic illustration of these measurements is presented in Fig. 7.

In principle deep inelastic lepton scattering containing a measured jet can provide a very clear test of the BFKL dynamics at low x [60, 61, 63]. The idea is to study deep inelastic (x, Q^2) events which contain an identified jet (x_j, k_{Tj}^2) where $x << x_j$ and $Q^2 \approx k_{Tj}^2$. Since we choose events with $Q^2 \approx k_{Tj}^2$ the leading order QCD evolution (from k_{Tj}^2 to Q^2) is neutralized and attention is focussed on the small x, or rather small x/x_j behaviour. The small x/x_j behaviour of jet production is generated by the gluon radiation as shown in the diagram of Fig. 7a. Choosing the configuration $Q^2 \approx k_{Tj}^2$ we eliminate by definition gluon emission which corresponds to strongly ordered transverse momenta i.e. that emission which is responsible for the LO QCD evolution. The measurement of jet production in this configuration may therefore test more directly the $(x/x_j)^{-\lambda}$ behaviour which is generated by the BFKL equation where the transverse momenta are not ordered. The recent H1 results concerning deep inelastic plus jest events are consistent with the increase of the cross-section with decreasing x as predicted by the BFKL dynamics [64].

A conceptually similar process is that of the two-jet production, with the jets separated by a large rapidity gap Δy, in hadronic collisions or in photoproduction as illustrated in Fig. 7c [65, 66]. Besides the characteristic $exp(\lambda \Delta y)$ dependence of the two-jet cross-section one expects significant weakening of the azimuthal back-to-back correlations of the two jets. This is the direct consequence of the absence of transverse momentum ordering along the gluon chain in the diagram of Fig. 7c.

Another measurement which should be sensitive to the QCD dynamics at small x is that of the transverse energy flow in deep inelastic lepton scattering in the central re-

gion away from the current jet and from the proton remnant as illustrated in Fig. 7b. [67]. The BFKL dynamics predicts in this case a substantial amount of transverse energy which should increase with decreasing x. The experimental data are consistent with this theoretical expectation [64]. Absence of transverse momentum ordering also implies weakening of the back-to-back azimuthal correlation of dijets produced close to the photon fragmentation region (see Fig. 7d) [68, 69].

6. Summary and conclusions

In this talk we have briefly described the QCD expectations for deep inelastic lepton scattering at low x which follow from the BFKL dynamics. It leads to the indefinite increase of gluon distributions with decreasing x which is correlated with the diffusion of transverse momenta. This increase of gluon distribution implies a similar increase of the structure functions through $g \to q\bar{q}$ transitions. Besides discussing the theoretical and phenomenological issues related to the description of the structure function F_2 at low x we have also emphasised the role of studying the hadronic final state in deep inelastic scattering.

The indefinite growth of parton distributions cannot go on forever and has to be eventually stopped by parton screening which leads to the parton saturation. Most probably, however, the saturation limit is still irrelevant for the small x region which is now being probed at HERA.

We have also discussed the small x behaviour of the spin dependent structure function g_1 focussing for simplicity on its non-singlet component which, at small x , can be (approximately) described by ladder diagrams with the quark (antiquark) exchange. The novel feature in this case is the appearance of double logarithmic terms i.e. contributions which contain powers of $\alpha_s ln^2(1/x)$. The perturbative QCD effects become significantly amplified for the singlet spin structure function due to mixing with the gluons. The simple ladder equation may not however be applicable for an accurate description of the double logarithmic terms in the polarized gluon distribution ΔG.

We have limited ourselves to the large Q^2 region where perturbative QCD is expected to be applicable. Specific problems of the low Q^2, low x region are discussed in ref. [70]. Finally let us point out that the change of the dynamics with the relevant scale is clearly visible in the data (see Fig. 1) and its satisfactory explanation is perhaps one of the most challenging problems of to-day.

Acknowledgments

I thank Robin Devenish and Mike Whalley for organizing an excellent meeting. I thank Barbara Badełek, Krzysztof Golec-Biernat, Alan Martin and Peter Sutton for most enjoyable research collaborations on the problems presented in this lecture. I am grateful to Grey College and to Physics Department of the University of Durham for their warm hospitality. This research has been supported in part by the Polish State Committee for

Scientific Research grant 2 P03B 231 08 and the EU under contracts n0. CHRX-CT92-0004/CT93-357.

References

[1] L.N. Gribov, E.M. Levin and M.G. Ryskin, Phys. Rep. **100** (1983) 1.

[2] B. Badełek et al., Rev. Mod. Phys. **64** (1992) 927.

[3] A.D. Martin, Acta. Phys. Polon, **B25** (1994) 265.

[4] J. Kwieciński, Nucl. Phys. B (Proc. Suppl.) **39 B,C** (1995) 58.

[5] E.A. Kuraev, L.N.Lipatov and V.S. Fadin, Zh. Eksp. Teor. Fiz. **72** (1977) 373 (Sov. Phys. JETP **45** (1977) 199); Ya. Ya. Balitzkij and L.N. Lipatov, Yad. Fiz. **28** (1978) 1597 (Sov. J. Nucl. Phys. **28** (1978) 822); J.B. Bronzan and R.L. Sugar, Phys. Rev. **D17** (1978) 585; T. Jaroszewicz, Acta. Phys. Polon. **B11** (1980) 965.

[6] L.N. Lipatov, in "Perturbative QCD", edited by A.H. Mueller, (World Scientific, Singapore, 1989), p. 441.

[7] A.J. Askew et al., Phys. Rev. **D47** (1993) 3775; Phys. Rev. **D49** (1994) 4402.

[8] H1 collaboration: A. de Roeck et al., preliminary measurements to be published in the Proc. of the Workshop on DIS and QCD, Paris, 1995, DESY preprint 95 - 152.

[9] ZEUS collaboration: B. Foster, to be published in the Proc. of the Workshop on DIS and QCD, Paris, 1995, DESY preprint 95-193.

[10] A. Donnachie and P.V. Landshoff, Phys. Lett. **B296** (1992) 257.

[11] P.D.B. Collins, "An Introduction to Regge Theory and High Energy Physics", Cambridge University Press, Cambridge, 1977.

[12] B.L. Ioffe, V.A. Khoze and L.N. Lipatov, "Hard Processes", North Holland, Amsterdam-Oxford-NewYork-Tokyo, 1984.

[13] J. Ellis and M. Karliner, Phys. Lett. **B231** (1988) 72.

[14] A. Donnachie and P.V. Landshoff, Z. Phys. **C61** (1994) 161.

[15] A. Levy, these proceedings.

[16] M. Ciafaloni, Nucl. Phys. **B296** (1988) 49.

[17] S. Catani, F. Fiorani and G. Marchesini, Phys. Lett. **B234** (1990) 339; Nucl. Phys. **B336** (1990) 18; G. Marchesini, in Proceedings of the Workshop "QCD at 200 TeV", Erice, Italy, 1990, edited by. L. Cifarelli and Yu. L. Dokshitzer (Plenum Press, New York, 1992), p. 183; G. Marchesini, Nucl. Phys. **B445** (1995) 49.

[18] J. Kwieciński, A.D. Martin, P.J. Sutton, Phys. Rev. **D52** (1995) 1445.

[19] B. Andersson, G. Gustafson and J. Samuelsson, Lund preprint LU TP 95-13.

[20] Yu.L. Dokshitzer et al., Rev. Mod. Phys. **60** (1988) 373.

[21] S. Catani, M. Ciafaloni and F. Hautmann, Phys. Lett. **B242** (1990) 97; Nucl. Phys. **B366** (1991) 657; J.C. Collins and R.K. Ellis, Nucl. Phys. **B 360** (1991) 3; S. Catani and F. Hautmann, Nucl. Phys. **B427** (1994) 475.

[22] M. Ciafaloni, Phys. Lett. **356** (1995) 74.

[23] J. Kwieciński, A.D. Martin, Phys. Lett. **B353** (1995) 123.

[24] T. Jaroszewicz, Phys. Lett. **B116** (1982) 291.

[25] A.D. Martin, J. Kwieciński and P.J. Sutton, Nucl. Phys. B (Proc. Suppl.) **A29** (1992) 67.

[26] J.C. Collins, P.V. Landshoff, Phys. Lett. **B276** (1992) 196.

[27] J.F. McDermott, J.R. Forshaw and G.G. Ross, Phys. Lett. **B349** (1995) 189.

[28] R.K. Ellis, Z. Kunszt and E.M. Levin, Nucl. Phys. **B420** (1994) 517; Erratum-ibid. **B433** (1995) 498.

[29] R.K. Ellis, F. Hautmann and B.R. Webber, Phys. Lett. **B348** (1995) 582.

[30] R.D. Ball and S. Forte, Phys. Lett. **351** (1995) 313.

[31] J.R. Forshaw, R.G. Roberts and R.S. Thorne, Phys. Lett. **B356** (1995) 79.

[32] J. Kwieciński, A.D.Martin and P.J. Sutton, Durham preprint DTP/95/94.

[33] A.D. Martin, R.G. Roberts and W.J. Stirling, Phys. Rev. **D50** (1994) 6734; Phys. Lett. **354** (1995) 155.

[34] M. Glück, E. Reya and A. Vogt, Z.Phys. **C67** (1995) 433.

[35] A. de Rujula et al., Phys. Rev. **D10** (1974) 1649.

[36] L.N. Lipatov, Nucl. Phys. **B452** (1995) 969; talk given at the International Conference on Elastic and Diffractive Scattering, "Frontiers in Strong Interactions", Chateau de Blois, France, June 1995.

[37] R. Kirschner, L.N. Lipatov and L. Szymanowski, Nucl. Phys. **B425** (1994) 579; Phys. Rev. **D51** (1995) 838.

[38] L.D. Fadeev and G.P. Korchemsky, Phys. Lett. **B342** (1995) 311; G.P. Korchemsky, to be published in the Proc. of the Workshop on DIS and QCD; G.P. Korchemsky, Stony Brook preprint ITP-SB-95-25; R. Janik, Cracow preprint TPJU-18-95.

[39] A.H. Mueller and W.K. Tang, Phys. Lett. **B284** (1992).

[40] J. Bartels et al., Phys. Lett. **B348** (1995) 589.

[41] J. Bartels, M. Wüsthoff, Z. Phys. **C66** (1995) 157; J.. Bartels, L.N. Lipatov and M. Wüsthoff, DESY preprint 95-171.

[42] A.H. Mueller, Nucl. Phys., **B415** (1994) 373; A.H. Mueller and B. Patel, Nucl. Phys. **B425** (1994) 471; A.H. Mueller, Nucl. Phys. **B437** (1995) 107; Chen Zhang and A.H. Mueller, Nucl. Phys. **B451** (1995) 579.

[43] V.S. Fadin, talk given at the International Conference on Elastic and Diffractive Scattering, "Frontiers in Strong Interactions", Chateau de Blois, France, June 1995.

[44] A.R. White, talk given at the International Conference on Elastic and Diffractive Scattering, "Frontiers in Strong Interactions", Chateau de Blois, France, June 1995.

[45] V.G. Gorshkov et al., Yad. Fiz. **6** (1967) 129 (Sov. J. Nucl. Phys. **6** (1968) 95); L.N. Lipatov, Zh. Eksp. Teor. Fiz. **54** (1968) 1520 (Sov. Phys. JETP **27** (1968) 814).

[46] J. Kwieciński, Phys. Rev. **D26** (1982) 3293.

[47] R. Kirschner and L.N. Lipatov, Nucl. Phys. **B213** (1983) 122.

[48] B.I. Ermolaev, S.I. Manayenkov and M.G. Ryskin, DESY preprint 95-017.

[49] J. Bartels, B.I. Ermolaev and M.G. Ryskin, DESY preprint 95 - 124.

[50] M.A.Ahmed and G.G. Ross, Phys. Lett. **B56** (1975) 385; Nucl. Phys. **B11** (1976) 298; G. Altarelli and G. Parisi, Nucl. Phys. **B126** (1977) 298.

[51] R.D. Ball, S. Forte and G. Ridolfi, Nucl. Phys. **B444** (1995) 287.

[52] J. Kwieciński, Durham preprint DTP 95/98 (to appear in Acta Physica Polonica).

[53] C. Bourrely and J. Soffer, Phys. Rev. **D51** (1995) 2108; Nucl. Phys. **B445** (1995) 341; Marseille preprint CPT-95/P.3224.

[54] M. Glück, E. Reya and W. Vogelsang, Phys. Lett. **B359** (1995) 201.

[55] T. Gehrmann and W.J. Stirling, Durham preprint DTP/95/62.

[56] J. Blümlein and A. Vogt, DESY preprint 95-175.

[57] S.D. Bass, P.V. Landshoff, Phys. Lett. **B336** (1994) 537.

[58] F.E. Close, R.G. Roberts, Phys. Lett. **B336** (1994) 257.

[59] A.D. Martin, review talk presented at the Blois Workshop "The Heart of the Matter", June 1994, Blois, France.

[60] A.H. Mueller, J. Phys. **G17** (1991) 1443.

[61] J. Bartels, M. Loewe and A. DeRoeck, Z. Phys. **C54** (1992) 635.

[62] W.K.Tang, Phys. Lett. **B278** (1992) 363.

[63] J. Kwieciński, A.D. Martin and P.J. Sutton, Phys. Rev. **D46** (1992) 921; Phys. Lett. **B287** (1992) 254.

[64] H1 Collaboration, DESY preprint 95 - 108.

[65] V. del Duca, Phys. Rev. **D49** (1994) 4510.

[66] W.J. Stirling, Nucl. Phys. **B423** (1994) 56.

[67] J. Kwieciński, A.D. Martin, P.J. Sutton and K.Golec-Biernat, Phys. Rev. **D50** (1994) 217; K.Golec-Biernat, J. Kwieciński, A.D. Martin and P.J. Sutton, Phys. Lett. **B335** (1994) 220.

[68] J.R. Forshaw and R.G. Roberts, RAL preprint 94-0228.

[69] A.J. Askew et al., Phys. Lett. **B338** (1994) 92.

[70] B. Badełek and J. Kwieciński, Warsaw preprint IFD/1/94 (to appear in Rev. Mod. Phys.).

Figure captions

1. The total virtual photon cross-section plotted as a function of W^2 for different values of the photon virtuality Q^2. The curves correspond to the theoretical parametrizations [34, 14]. In particular the skewed curve is the GRV prediction for $Q^2 = 0.35GeV^2$. The figure is taken from ref. [15].

2. Diagrammatic representation of the BFKL equation (6).

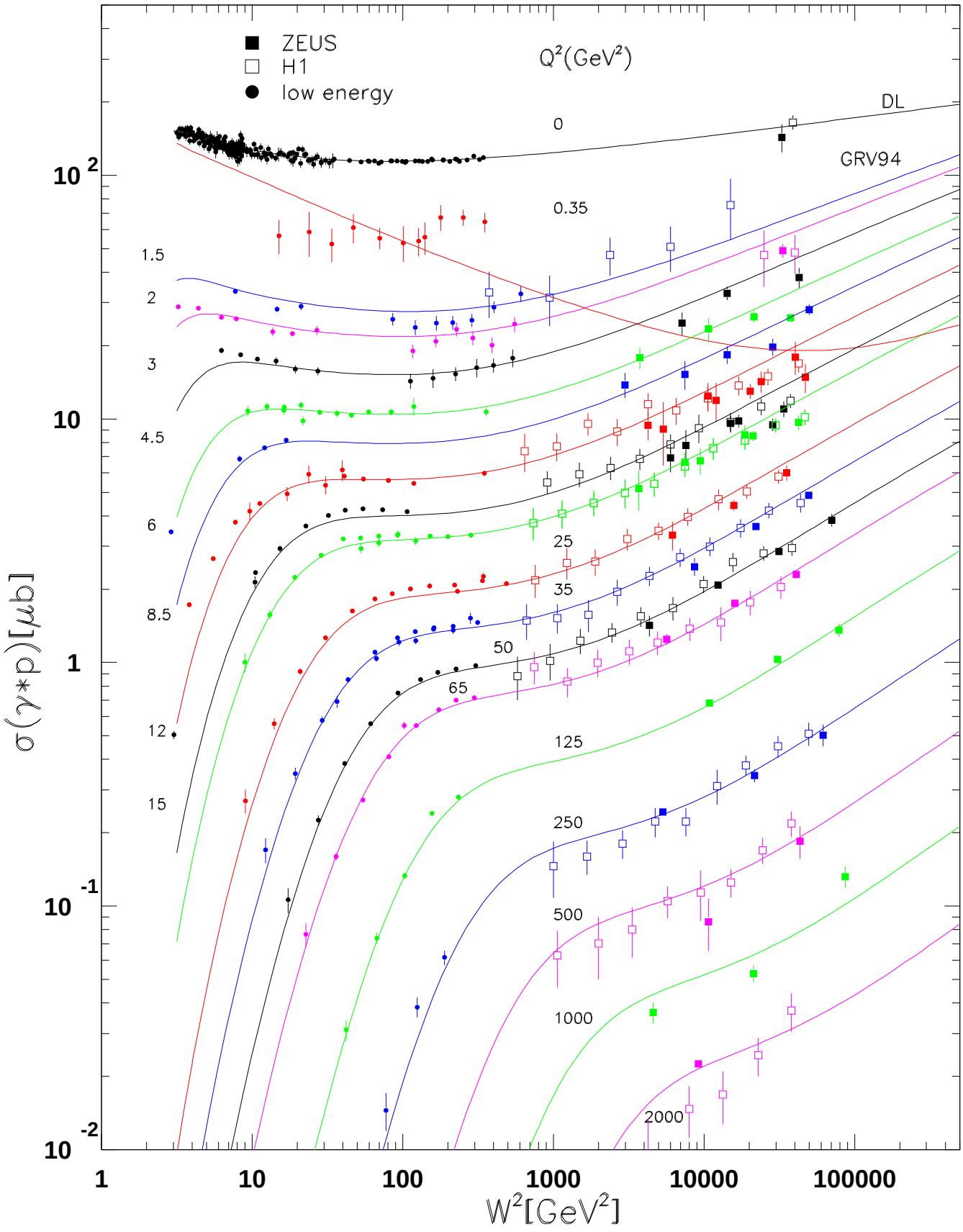
3. Diagrammatic representation of the k_t factorization formula (26).

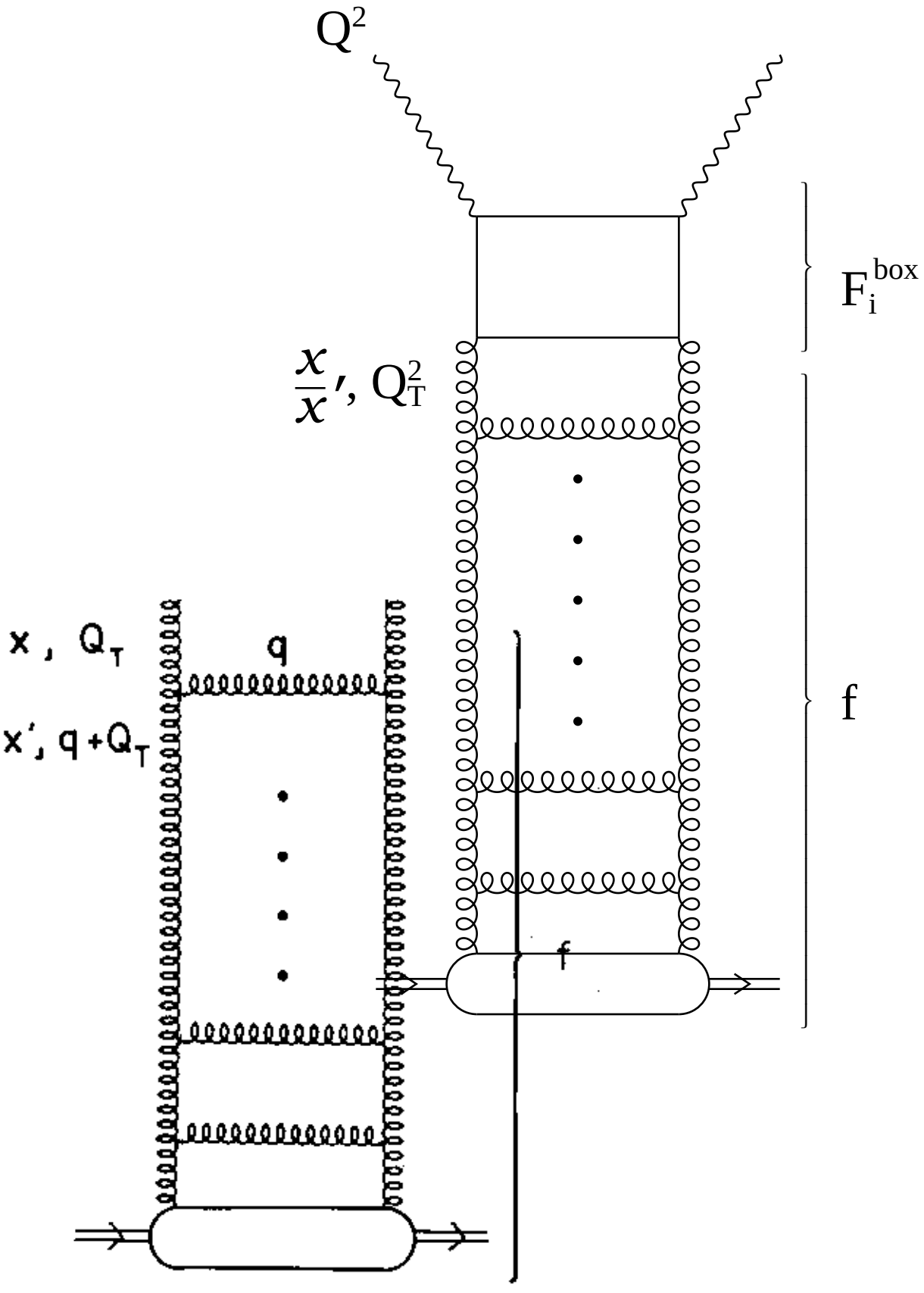
4. Theoretical predictions for the structure function $F_2(x, Q^2)$ based on the Altarelli-Parisi evolution equations with the leading $ln(1/x)$ terms resummed in both the P_{gg} and P_{qg} splitting functions (solid and dotted curves where the dotted curve is based on the different prescription for imposing the momentum sum rule). The dot-dashed curves show predictions when the leading $ln(1/x)$ resummation is included only in the splitting function P_{gg}. The dashed curves correspond to the two-loop prediction. The theoretical curves are confronted with the 1993 data from HERA. The figure is taken from ref. [29].

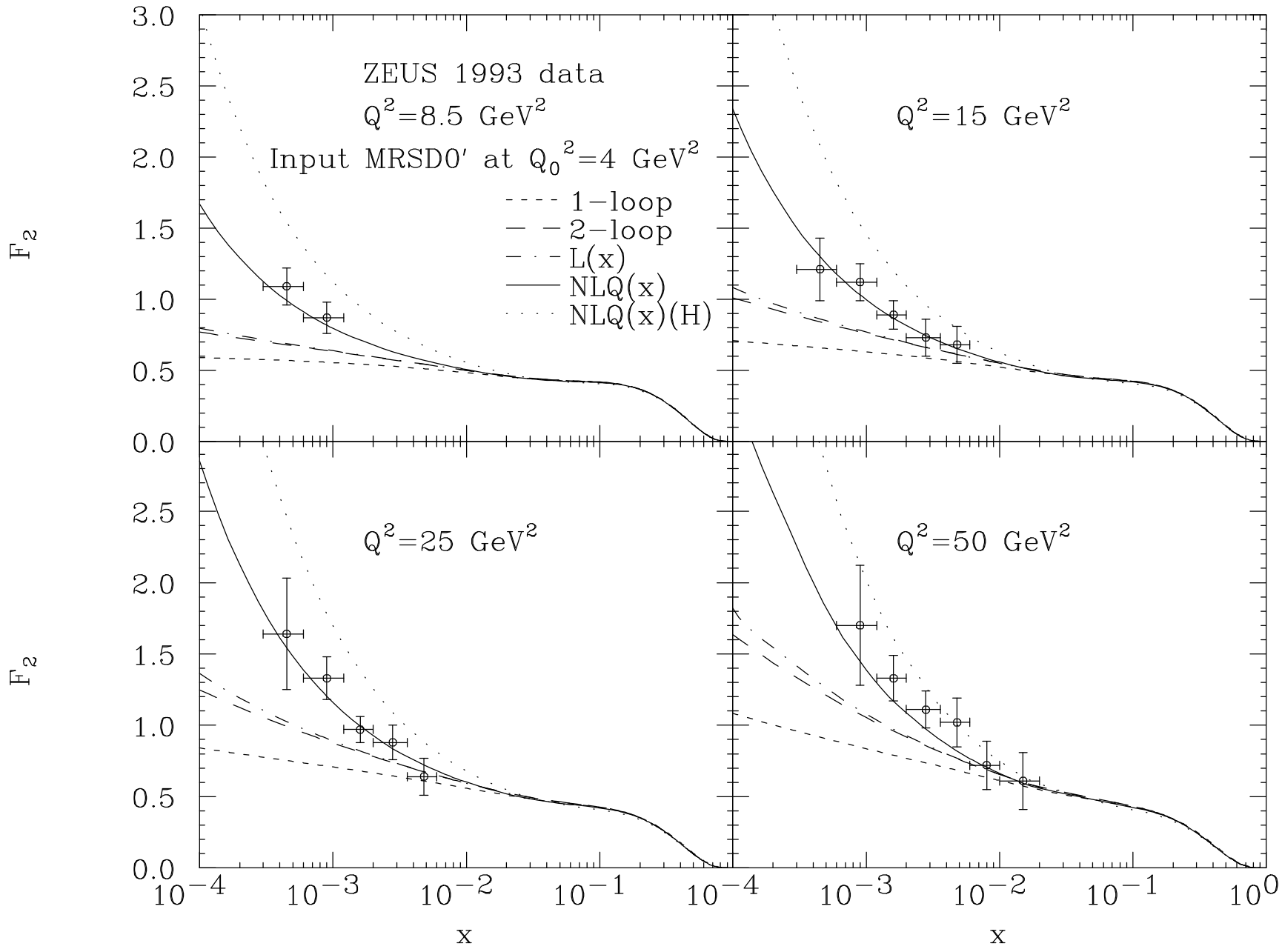
5. A comparison of the HERA measurements of F_2 [8, 9] with the predictions based on the k_t factorization formula (26) using for the unintegrated gluon distributions f the solutions of the CCFM equation (30) (continuous curve) and of the approximate form of this equation corresponding to setting $\Theta(Q - q)$ in place of $\Theta(Q - qx/x')$ and $\Delta_R = 1$ (dotted curve). We also show the values of F_2 obtained from collinear factorization using MRS(A′) [33] and GRV [34] partons (the figure is taken from ref. [32]).

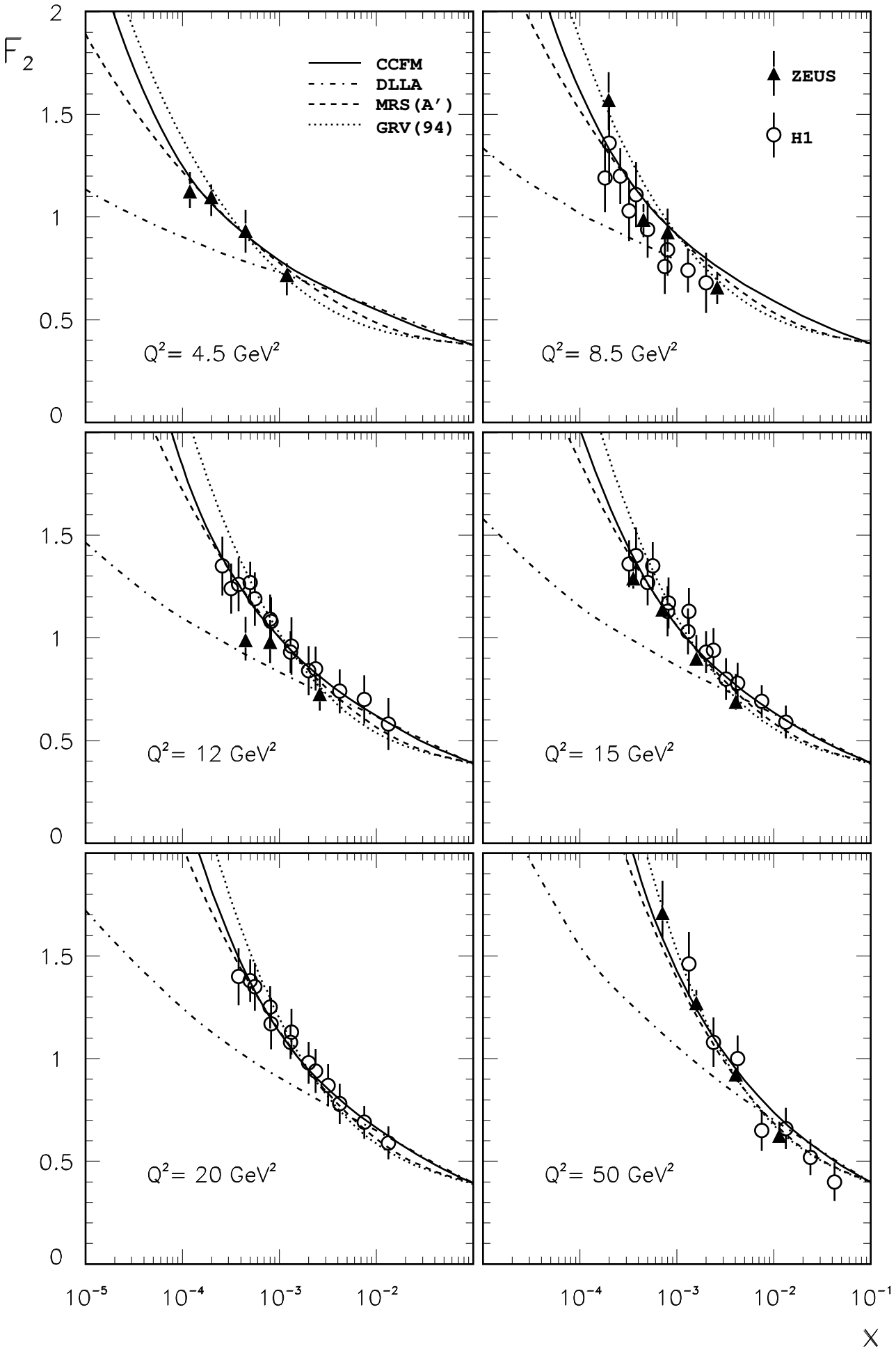
6. The ladder diagram with quark (antiquark) exchange.

7. Diagrammatic representation of the processes testing BFKL dynamics. (a) Deep inelastic scattering with the forward jet. (b) E_T flow in deep inelastic scattering. (c) Production of jets separated by the large rapidity gap Δy. (d) Dijet production in deep inelastic scattering (the figure is taken from ref. [59]).


ZEUS
H1
low energy
$Q^2(GeV^2)$
DL
GRV94
0
0.35
1.5
2
3
4.5
6
8.5
12
15
25
35
50
65
125
250
500
1000
2000
$\sigma(\gamma^* p)[\mu b]$
$W^2[GeV^2]$
10^2
10
1
10^{-1}
10^{-2}
1
10
100
1000
10000
100000


Q^2
F_i^{box}
$\frac{x}{x'}, Q_T^2$
f
x , Q_T
q
x', q+Q_T
f


ZEUS 1993 data
Q^2=8.5 GeV^2
Input MRSD0′ at $Q_0{}^2$=4 GeV^2
1−loop
2−loop
L(x)
NLQ(x)
NLQ(x)(H)
Q^2=15 GeV^2
Q^2=25 GeV^2
Q^2=50 GeV^2
F_2
F_2
x
x
3.0
2.5
2.0
1.5
1.0
0.5
0.0
10^{-4}
10^{-3}
10^{-2}
10^{-1}
10^{0}


F_2
CCFM
DLLA
MRS(A')
GRV(94)
ZEUS
H1
Q^2= 4.5 GeV^2
Q^2= 8.5 GeV^2
Q^2= 12 GeV^2
Q^2= 15 GeV^2
Q^2= 20 GeV^2
Q^2= 50 GeV^2
0
0.5
1
1.5
2
10^{-5}
10^{-4}
10^{-3}
10^{-2}
10^{-1}
x